Available online www.ejaet.com

European Journal of Advances in Engineering and Technology, 2024, 11(6):1-10

Research Article ISSN: 2394 - 658X

Numerical Study of the Effect of the Rayleigh Number on the Magneto Convection of A Newtonian Fluid Confined Between Two Vertically Eccentric Hemispheres

Fallou Sarr*, Vieux Boukhaly Traore, Omar Ngor Thiam and Mamadou Lamine Sow

Fluid Mechanics, Hydraulics and Transfers Laboratory, Department of Physics, Faculty of Science and Technology, Cheikh Anta DIOP University, Dakar, Senegal
Email : sarrgalass6@gmail.com

ABSTRACT

This work contributes to the numerical study of laminar natural convection of an electrically conductive Newtonian fluid subjected to a uniform oblique magnetic field. The study focuses on a hemispherical cavity bounded by two vertically eccentric hemispheres. The inner hemisphere is subjected to a constant heat flux while the outer hemisphere is maintained at a fixed temperature. Thermal and electrical boundary conditions are combined to determine the critical values of parameters indicating the onset of instability. The Boussinesq approximation is used to analyze the equations governing this fluid instability. These equations are projected onto the bispherical coordinate system and discretized using the finite difference method, allowing for the development of a FORTRAN code. Using this code, growth rates are calculated for different values of the Rayleigh number (ranging from 103 to 107), Hartmann number (0.01), eccentricity (0.2), the ratio of radii (2), and the inclination angle of the magnetic field. The study demonstrates that the Rayleigh number has a significant impact on the magnetoconvection of a Newtonian fluid confined between two vertically eccentric hemispheres by regulating the intensity and complexity of convective movements in the fluid.

Keywords: Magnetoconvection, Magnetic field, Hemispherical cavity, Rayleigh correlations, Hartmann number

---

INTRODUCTION

The physical phenomenon that describes the convective movement of an electrically conductive fluid subjected simultaneously to convection and magnetic forces, commonly known as magnetoconvection, has been extensively studied in recent decades [1]. The significance of this phenomenon lies in its relevance to numerous applications in various research fields [2], such as astrophysics, geophysics, engineering, and metallurgy. It is also used to study phenomena such as solar flares, ocean currents, and nuclear fusion processes [3]. Alongside the issues of pure natural convection, various experimental and numerical approaches to magnetoconvection of a fluid confined in enclosures have been addressed [4]. In these studies, the enclosure configurations are typically varied and can sometimes be parallelepipedal [5, 6], cylindrical [7, 8], or even spherical [9, 10, 11, 12]. These studies have proposed correlations between the Nusselt and Rayleigh numbers, which are influenced by wall geometry, fluid viscosity, and flow stability [13, 14]. Modeling a magnetoconvection problem proves that the discretization method, as well as grid refinement and stretching, stabilize the primary convection roll, and the horizontal magnetic field also results in higher kinetic energy and heat transfer rates compared to a non-magnetic case [6]. Another study analyzed the Hall effects on magnetoconvective instability and heat transfer, showing that Hall currents reduce the flow field [15]. Research has also been conducted to understand the characteristics of flow and heat transfer in an enclosure in the presence of a magnetic field, showing that the magnetic field decreases the heat transfer rate [16, 17]. Another aspect studied by [18] is mixed convection, with an exponential temperature distribution in the presence of a magnetic field and internal thermal and viscous dissipation. The results showed that an increase in the Prandtl number decreases the skin friction coefficient, while an increase in the magnetic field enhances the local Nusselt number. A study by [9] examined the natural convection of a non-conductive Newtonian fluid between two vertically eccentric spheres, showing that an increase in the modified Rayleigh number allows reaching a steady

state more quickly and that the influence of eccentricity is weak. The convection motion is strengthened for positive eccentricities, and the heat exchange increases with the modified Rayleigh number. [19] also studied the case of a hemisphere, showing that the vortex center moves upward for higher eccentricities, and the Nusselt number increases with the modified Rayleigh number. A study proposed by [20] focuses on the thermal convection of an electrically conductive fluid subjected to a magnetic field. Such abundant literature gives significant importance and scientific scope to the study of heat transfer. In fact, this motivated the initiation of the present study. It concerns natural convection between two vertically eccentric hemispheres of a conducting fluid subjected to a magnetic field. The aim is to study, for a transient flow regime, the magnetoconvection of a Newtonian fluid subjected to an oblique magnetic field and confined between two vertically eccentric hemispheres. To do this, a constant heat flux is imposed on the inner hemisphere while the outer hemisphere is maintained at a constant temperature. The main objective is, on the one hand, to determine the influence of the Rayleigh number on the isotherms and streamlines, and on the other hand, its influence on the Nusselt number, the stream function, and the temperature.

PROBLEM FORMULATION

The diagram shown in Figure 1 illustrates the displacement of a conducting fluid (moist air), which is a Newtonian fluid, subjected to an oblique magnetic field. This fluid is confined in an annular space bounded by two vertically eccentric hemispheres. The radii of the inner and outer hemispheres are denoted Ri and Re, respectively. The distance between the centers of these two hemispheres is defined by the eccentricity e'. Initially, the temperature inside and on the walls of the enclosure is uniform. A constant heat source (q') is applied to the inner hemisphere, while the temperature of the outer hemisphere remains constant (T'). The walls separating the two hemispheres at angles $\theta = 0$ and $\theta = \pi$ are adiabatic.

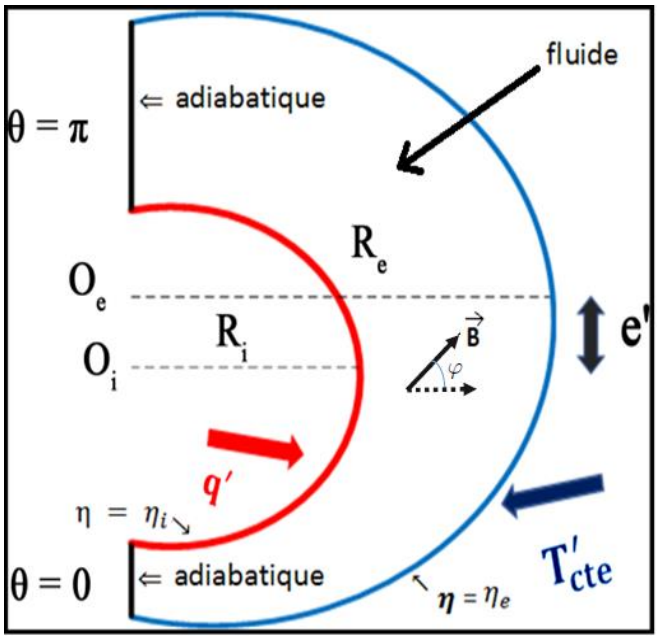

Fig. 1: Problem geometry

A transient natural convection of the conductive fluid will develop within this space due to the temperature difference between the two hemispheres. The physical properties of the fluid remain constant, except for its density, which varies linearly with temperature and follows Boussinesq's law in the equation of motion. Fluid flow is laminar, incompressible and two-dimensional, and the magnetic field is assumed to be constant with neglect of the induced field. We also neglect the viscous dissipation function, radiative effects and the pressure term. The boundaries of the system under study are electrically insulating. The walls of our enclosure are made up of two spherical parts and two others offset from the vertical. To simplify the boundary conditions, it is necessary to use a curvilinear coordinate system in which the boundaries of our domain are parametrized by constant coordinate lines. Thus, given the geometry of the enclosure, the most appropriate coordinate system is that of bispherical coordinates. In the case of two-dimensional flow, relationship (1) allows us to pass from Cartesian coordinates (x, y) to bispherical coordinates:

$$\begin{cases} x = \frac{a \sin\theta}{ch\eta - cos\theta} \\ y = \frac{a\, sh\eta}{ch\eta - cos\theta} \end{cases} \quad (1)$$

Along the vertical are two walls identified by θ = 0 and θ = π. The two inner and outer hemispheres are respectively materialized by the coordinate lines h=hi and h=hi.

BASIC EQUATIONS

After introducing the simplifying assumptions, we establish the various dimensionless equations necessary for solving the problem considered in this study. The vorticity-flux functions (vortical flow) are represented by the momentum and heat equations, which are expressed by the relation (2):

$$\partial_t F + A(U)\partial_\eta F + B(V)\partial_\theta F = P\left(\partial_\eta^2 F + \partial_\theta^2 F\right) + S\left(G_2\partial_\eta T - G_1\partial_\theta T\right) + R\left(\partial_\eta B_1 - \partial_\theta B_2\right) \quad (2)$$

The different values of the variables F, A, B, P, S and G are given in Table 1.

Table 1: Variables in the heat and vorticity equation

Equation	*F*	A(U)	B(V)	P	S	R
Heat	T	$\frac{1}{H}\left[U - \frac{G_2}{K}\right]$	$\frac{1}{H}\left[V + \frac{G_1}{K}\right]$	$\frac{1}{H^2}$	0	0
Movement	$\frac{\Omega}{K}$	$\frac{1}{H}\left[U - \frac{3PrG_2}{K}\right]$	$\frac{1}{H}\left[V + \frac{3PrG_1}{K}\right]$	$\frac{Pr}{H^2}$	$\frac{Ra.Pr}{KH}$	$\frac{Ha^2.Pr}{KH^2}$

With:

$$\begin{cases} B_1 = H\left(UB_\eta B_\theta - VB_\eta^2\right) \\ B_2 = H\left(VB_\eta B_\theta - UB_\theta^2\right) \end{cases} \quad (3)$$

$$\begin{cases} B_\eta = \frac{B_\eta^*}{B_0} = G_2\, cos\varphi + G_1\, sin\varphi \\ B_\theta = \frac{B_\eta^*}{B_0} = G_2\, sin\varphi - G_1\, cos\varphi \end{cases} \quad (4)$$

Where the quantities U, V, G_1, G_2, K, H, are defined by equations (5), (6) and (7).

$$\begin{cases} U = \frac{1}{HK}\,\partial_\theta\Psi \\ V = -\frac{1}{HK}\,\partial_\eta\Psi \end{cases} \quad (5)$$

$$\begin{cases} \mathrm{G_1} = \frac{1-\cos\theta\,\mathrm{ch}\eta}{\mathrm{ch}\eta-\cos\theta} \\ \mathrm{G_2} = -\frac{\sin\theta\,\mathrm{sh}\eta}{\mathrm{ch}\eta-\cos\theta} \end{cases} \quad (6)$$

$$\begin{cases} K = \frac{asin\theta}{D(ch\eta-cos\theta)} \\ H = \frac{a}{D(ch\eta-cos\theta)} \end{cases} \quad (7)$$

The condition of incompressibility is satisfied by the equation of the stream function given by relation (8):

$$\Omega = -\frac{1}{K^2H}\left(G_2\partial_\eta\Psi - G_1\partial_\theta\Psi\right) - \frac{1}{KH^2}\left(\partial_\eta^2\Psi + \partial_\theta^2\Psi\right) \quad (8)$$

In addition to these various equations, there are boundary conditions and initial conditions. At t = 0, the conditions are expressed by the relation (9):

$$\Omega=\Psi=T=U=V=0 \quad (9)$$

At t > 0, the boundary conditions are expressed by equations (10), (11), and (12) depending on the location of the wall.

- On the inner spherical wall ($\eta = \eta_i$)

$$\Psi = U = V = 0,\ \partial_\eta T = H_i = \frac{ch\eta_i}{sh^2\eta_i} \text{ and } \Omega = -\frac{1}{KH}\partial_\eta^2\Psi \quad (10)$$

- On the outer spherical wall ($\eta=\eta_e$)

$$\Psi = U = V = T = 0 \text{ and } \Omega = -\frac{1}{KH}\partial_\eta^2\Psi \quad (11)$$

- On both vertical walls ($\theta = 0$, $\theta = \pi$)

$$\Psi = U = V = \partial_\eta T = 0 \text{ and } \Omega = -\frac{1}{KH}\partial_\theta^2\Psi \quad (12)$$

The Nusselt number reflects the thermal energy transmitted by a spherical wall. The local Nusselt numbers, Nu, and the mean Nusselt number are defined by relations (13) and (14) depending on the wall.

For the inner spherical wall:

$$Nu_i = \frac{1}{T_{i,m}} \quad (13)$$

For the outer spherical wall:

$$Nu_e = \frac{1}{H_e T_{i,m}}\,\partial_\eta T \quad (14)$$

NUMERICAL METHOD

The transfer equations that govern our problem are non-linear and coupled partial differential equations. Due to their complexity, these equations are solved using numerical techniques. For the development of a numerical code simulating the magnetoconvection of a Newtonian fluid confined in an annular space, we used:

- The Alternating Direction Implicit (ADI) method for the temporal solution of the momentum and heat equations;
- The finite difference method for spatial integration.

We will use the Thomas algorithm to solve the system of linear equations obtained by the ADI method. However, for the flow function equation, the resolution is based on the successive over-relaxation (SOR) method with an optimal relaxation parameter. At the iterative loop level, the calculated result Znew of a quantity to be determined will only be considered as a convergent solution if it obeys the following relation (15) with the old value Zold:

$$\frac{|Z_{new}-Z_{old}|_{max}}{|Z_{new}|} \leq 10^{-5} \quad (15)$$

Steady state is reached only if this relative error between two consecutive time steps for all quantities obeys relation (16):

$$\frac{|Z^{n+1}-Z^{n}|_{max}}{|Z^{n+1}|_{max}} \leq 10^{-5} \quad (16)$$

Zn represents Ω, Ψ or T for the nth time step.

RESULTS AND DISCUSSIONS

In this section, we will examine the results and discussions arising from a comprehensive numerical study on the magnetoconvection of a Newtonian fluid subjected to various Rayleigh numbers.

CALCULATION CONDITIONS

The choice of a 51 x 51 mesh grid and a time step of 10^{-4} is motivated by tests conducted on their influence. The results of these tests are presented in tables 2 and 3 and prove that these choices represent, among other things, a good compromise.

Table 2: Effects of time steps on the Nusselt number of the thermal wall for Ha=1, Ra=10^5, e=0, Δt=10^{-4} and the grid system is 51x51

	Time steps		
	10^{-3}	**10^{-4}**	**10^{-5}**
Nu	4.7337	4.7298	4.7296
Difference (%)	0.087	0.004	0
Time computing (min)	5	124	802

Table 3: Effects of mesh refinement on the Nusselt number of the thermal wall forHa=1, Ra=10^5, e=0 and Δt=10^{-4}

	Mesh grid							
	21*21	21*41	41*41	41*51	41*81	51*51	51*81	81*81
Nu	4.8750	4.8871	4.7515	4.7503	4.7502	4.7298	4.7297	4.7060
Difference (%)	3.59	3.85	0.97	0.94	0.94	0.51	0.50	0
Time computing (min)	9	97	225	261	362	348	447	604

VALIDATION

When there is no magnetic field, the problem becomes one of natural laminar convection. The values of the mean Nusselt number are given in Table 4 for different Rayleigh numbers. We have compared these results with those of the study [19] on transient laminar convection between two vertically eccentric hemispheres. These comparisons show a relative difference of 02.72% for all cases studied, indicating excellent agreement between the results.

Table 4: Comparison of the average Nusselt number for e = 0

	Ra				
	10^3	**10^4**	**10^5**	**10^6**	**10^7**
Nusselt number (our results)	2.0673	3.0379	4.8920	7.7680	11.708
Nusselt number (results of [19])	2.125	3.0651	4.982	7.6874	11.671
Difference (%)	2.72	0.89	1.81	1.05	0.32

INFLUENCE OF THE RAYLEIGH NUMBER

To study the influence of the Rayleigh number on magnetoconvection, we will set the value of the eccentricity to; the Hartmann number Ha=0.01, and the inclination angle of the magnetic field.

Through figures 2, 3, 4, 5, and 6, we have presented the temporal evolution of the isotherms on the right and the streamlines on the left for different Rayleigh numbers ranging from 103 to 107.

For the Rayleigh number Ra=103, according to figure 2, the fluid circulates weakly. The isotherms are highly concentrated and circular in shape, following the inner spherical wall of the container. There is also a decrease in temperature from the hot spherical wall towards the cold wall. Over time, the evolution and parallelism of the isotherms decrease, indicating a pseudo-conductive regime.

When the Rayleigh number is 104 (figure 3), heat transfer through magnetic convection predominates over thermal conduction. This predominance of convection is manifested by the widening of the isotherm lines, as the temperature becomes more uniform as we move away from the hot spherical wall. The displacement of fluid particles is more significant in the upper part of the container due to the buoyancy opposing the gravitational force. The isotherms deform further in figures 4 and 5, indicating a significant presence of the radiative effect for Rayleigh numbers Ra=105 and Ra=106.

For Ra=107, the isotherms in figure 6 show more pronounced temperature gradients, making them more complex with areas of higher temperature associated with convection movements. The regime becomes pre-turbulent.

In general, we observe an upward movement of fluid particles that heat up near the hot inner spherical wall. Under the effect of buoyancy, they move upward along this wall, then descend near the cold outer spherical wall. This downward movement of particles creates a region of low velocity between these two wall-adjacent regions.

Regarding the streamlines, for Ra=103, the rotation center of the vortex moves slightly away from the heated inner spherical wall, as shown in figure 2. However, for Ra=104 and Ra=105, convection sets in and the rotation center rises higher above the inner spherical wall, approaching the outer wall, as shown in figures 3 and 4. These phenomena are due to the appearance of fluid movements, as the absolute value of the minimum of the stream function increases.

For Ra=106, convection becomes more significant, and figure 3 shows deformation of the vortex. Heated particles rise due to buoyancy, then cool down as they approach the hot outer spherical wall and descend under the effect of gravity.

In conclusion, for all values of the Rayleigh number, we observe a fluid movement from the heated inner spherical wall towards the hot outer wall of the container, opposing gravity. This phenomenon intensifies with increasing Rayleigh number.

Figure 6 clearly shows that for a Rayleigh number Ra=107, convection currents develop further and become more dynamic, with more complex and sinuous streamlines, forming vortex structures.

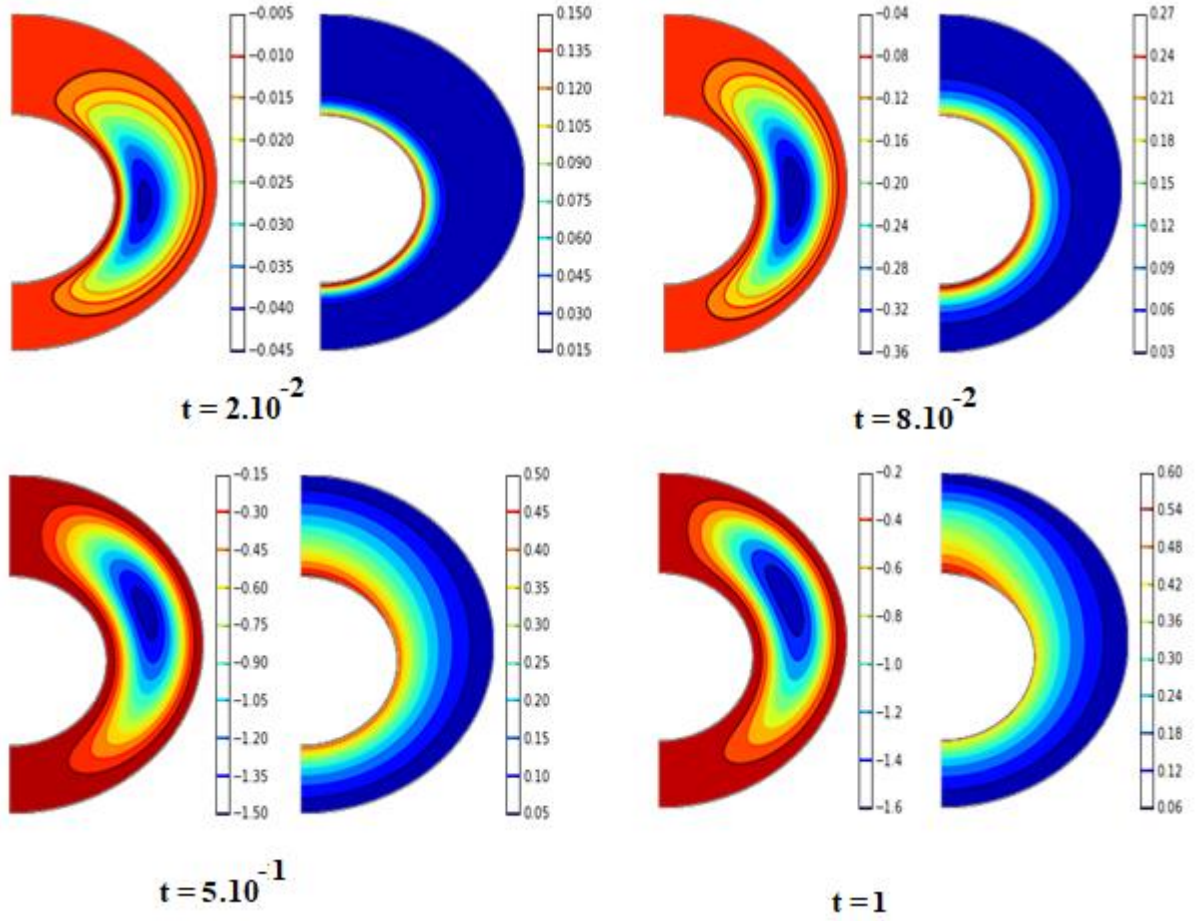

Fig. 2: Current lines and isotherms for $Ra=10^3$; e=0.2; Ha=0.01; $\varphi=\pi/6$

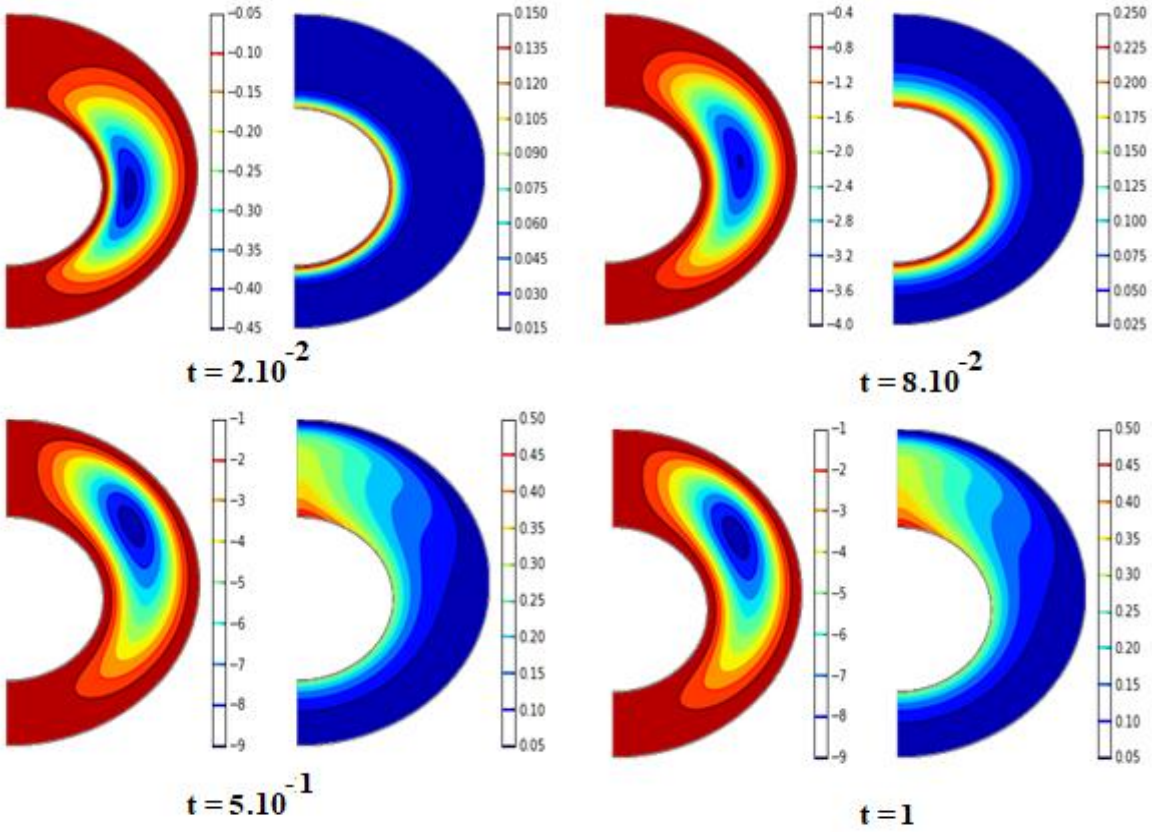

Fig. 3: Current lines and isotherms for Ra=104; e = 0.2; Ha=0.01; φ=π/6

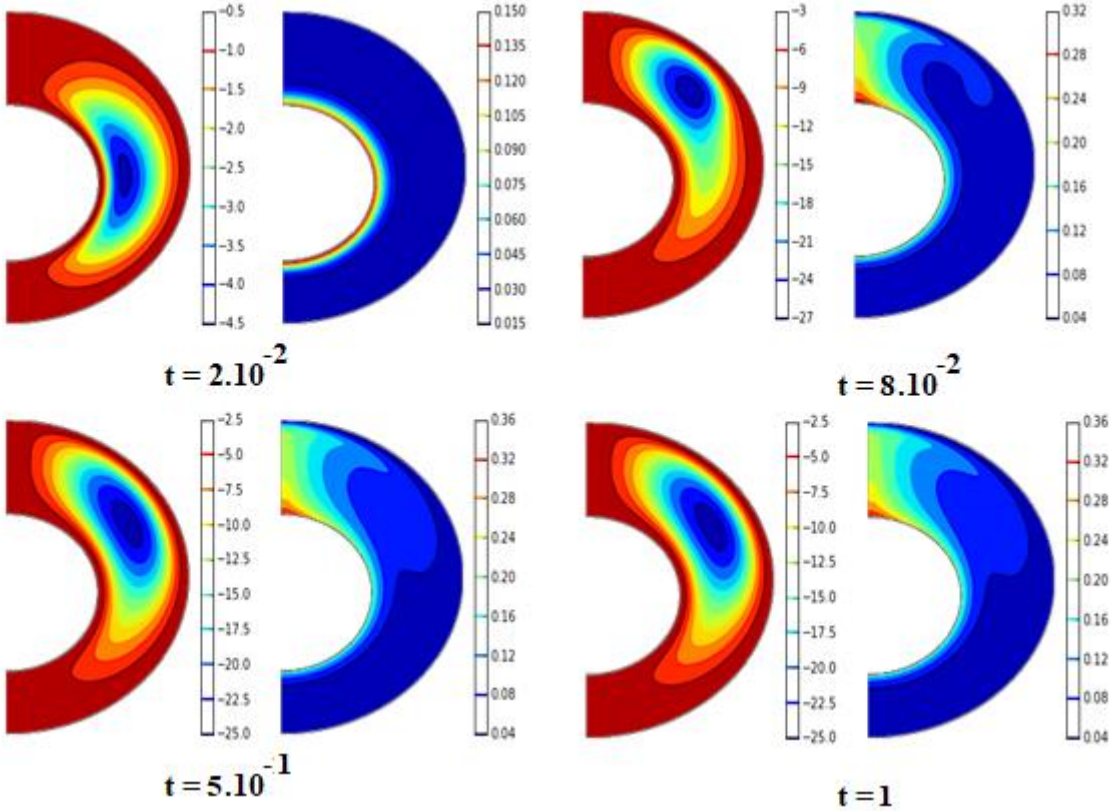

Fig. 4: Current lines and isotherms for Ra = 10^5; e = 0.2; Ha = 0.01; φ = π/6

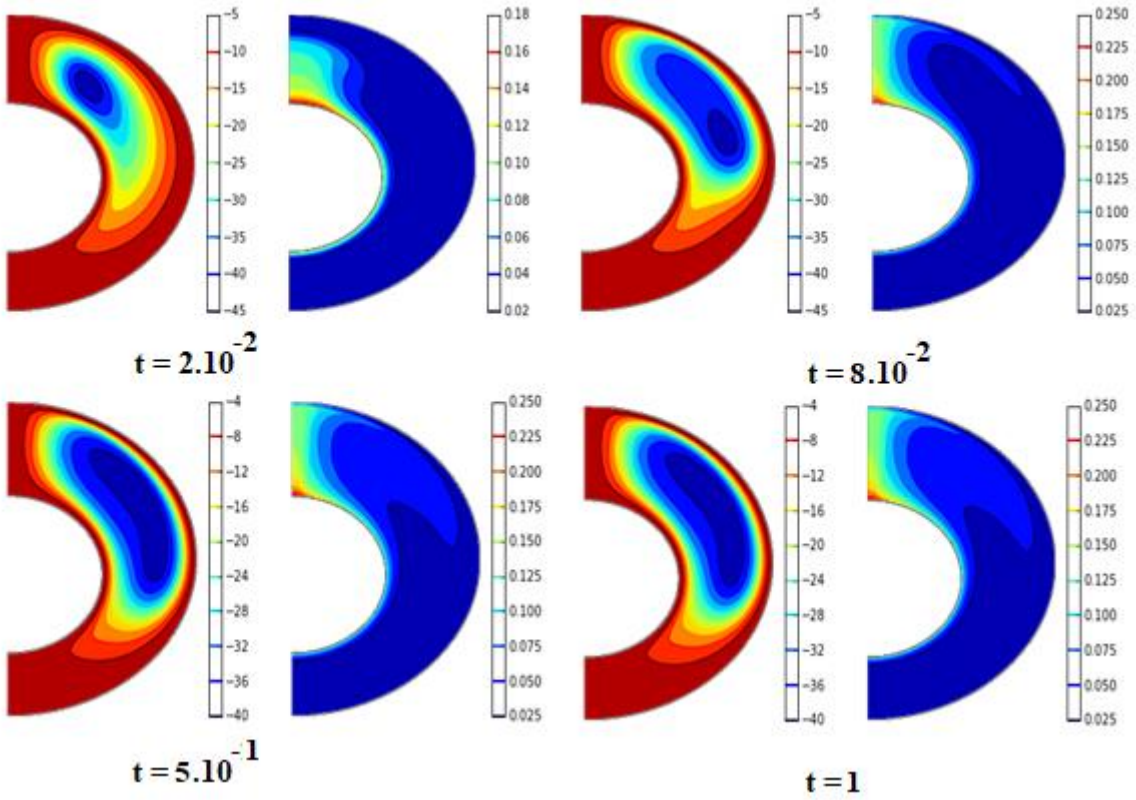

Fig. 5: Current lines and isotherms for Ra = 106; e = 0.2; Ha = 0.01; φ = π/6

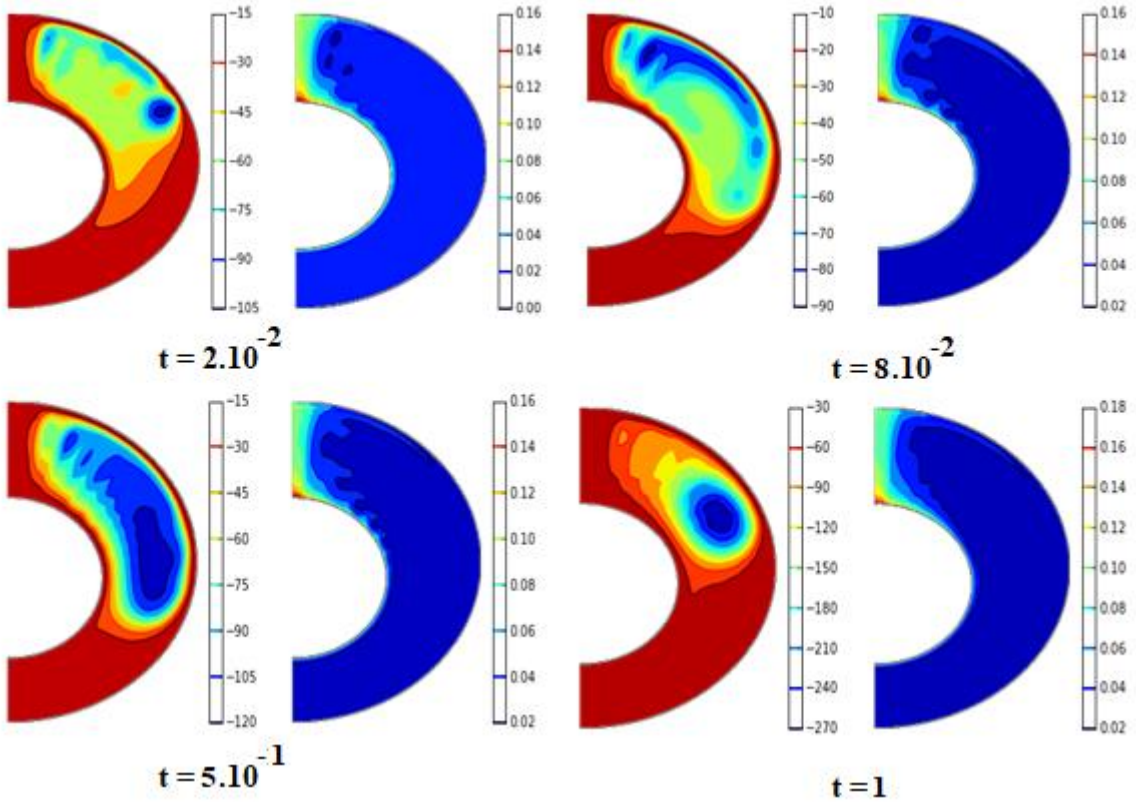

Fig. 6: Current lines and isotherms for Ra = 10^7; e = 0.2; Ha = 0.01; φ = π/6

MINIMUM CURRENT FUNCTION, NUSSELT NUMBER AND HEATED WALL TEMPERATURE

The curves in the graph 7 below illustrate the evolution, as a function of time, of the average Nusselt number on the heated inner wall, the average temperature of this wall, and the minimum stream function, for Rayleigh number values ranging from 10^3 to 10^7.

The evolution of the dimensionless average Nusselt number on the inner hemisphere with respect to time demonstrates a decrease followed by a monotonic phase. The increase in the Rayleigh number indicates an increase in convection and therefore an increased heat transfer, resulting in an increase in the Nusselt number.

The evolution of the dimensionless average temperature of the inner wall, for Rayleigh numbers ranging from 10^3 to 10^7, shows a temporal growth before stabilizing at a certain point. When the Rayleigh number is low ($Ra=10^3$), the temperature of the heated wall remains relatively constant and does not show significant variations. However, when the Rayleigh number increases beyond a critical value, i.e., starting from 10^4, the average temperature of the wall also increases.

For the same Rayleigh numbers, the evolution of the minimum stream function decreases rapidly with respect to dimensionless time, then stabilizes once the steady state is reached. This decrease is more pronounced for higher values of the Rayleigh number. If the Rayleigh number takes values of 10^5 and 10^6, the curves exhibit peaks before stabilizing. On the other hand, for a Rayleigh number equal to 10^7, the minimum stream function exhibits two peaks but struggles to stabilize: this is the pre-turbulent regime. The explanation for this phenomenon is that, initially, thanks to the initial conditions and system boundaries, magnetic convection predominates, leading to significant fluid movement. Once the steady state is reached, these magnetoconvective phenomena attenuate.

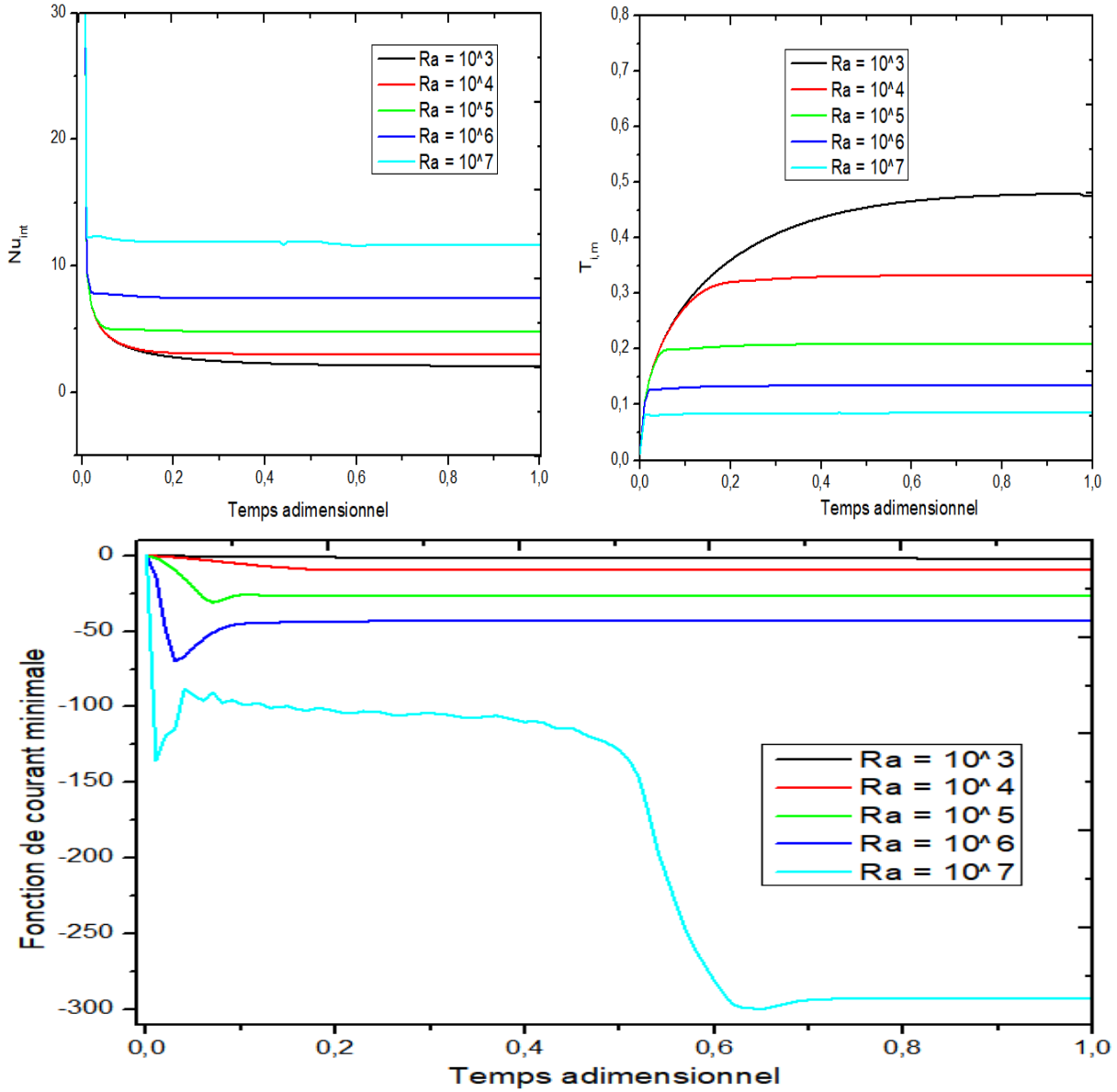

Fig. 7: Influence of Rayleigh number on various parameters

CONCLUSION

In this article, we conducted a numerical study of magnetoconvection in a fluid confined between two eccentric hemispheres. We subjected the hemispherical cavity to thermal and electrical boundary conditions to determine the critical values of parameters that mark the onset of instability. To do this, we imposed a constant heat flux density on the inner hemispherical wall and a constant temperature on the outer hemisphere. The equations governing magnetoconvection were projected into bispherical coordinates. After dimensionless scaling of our equations, spatial discretization was performed using finite difference methods. For temporal discretization, the equations were solved using the ADI and SOR methods.

For very weak magnetic fields, magnetoconvection simplifies into a natural convection problem. The results of our study are consistent and significant:

- For a Rayleigh number (Ra) equal to 103, which characterizes the conductive regime, and a low Hartmann number, the isotherms resemble eccentric circles following the inner hemispherical wall. When the Rayleigh number increases to Ra=104, Ra=105, and up to Ra=106, magnetoconvection becomes increasingly dominant. This dominance is manifested by a very pronounced deformation of the isotherms.
- The Rayleigh number also influences the Nusselt number, the minimum and maximum stream function values, and the temperature of the heated wall in a magnetoconvection problem. As Ra increases, heat transfer through convection becomes more efficient, currents become stronger, and the temperature of the heated wall decreases.

Acknowledgements

I am deeply grateful to my supervisor Mr Mamadou Lamine SOW, Professeur Titulaire, and my co-authors, in particular Mr Omar Ngor THIAM, Professeur Assimilé, for their collaboration and dedication in the accomplishment of our article. Their expertise and unfailing support were essential to its success.

NOMENCLATURE

a: torus pole parameter (m)
e: eccentricity
g: intensity of gravity ($m.s^{-2}$)
G_1 and G_2: coefficients
H and K: dimensionless metric coefficients
B_0: magnetic field strength ($N.A^{-1}.m^{-2}$)
Ha, Hartmann number
Nu_e, Nusselt number for the outer hemisphere
Nu_i, Nusselt number for inner hemisphere
O_i and O_e respectively center of inner and outer hemisphere
Pr, Prandtl number
q, heat flux density ($W.m^{-2}$)
R_i and R_e, radii of the inner and outer hemispheres respectively
Ra, Rayleigh number
t, dimensionless time
t', dimensional time (s)
T, dimensionless temperature
U and V, dimensionless velocity components in transformed planes
x and y, Cartesian coordinates, (m)
α, thermal diffusivity, ($m^2.s^{-1}$)
β, coefficient of thermal expansion, (K^{-1})
σ, electrical conductivity, ($A.m.V^{-1}$)
Δt, time step, (s)
ΔT, temperature difference between the two hemispheres, (K)
η and θ, bispherical coordinates, (m)
λ, thermal conductivity, ($W.K^{-1}.m^{-1}$)
ν, kinematic viscosity, ($m^3.s^{-1}$)
Ψ, dimensionless flux function,
Ψ′, dimensional flow function, ($m^3.s^{-1}$)
Ω, dimensionless vorticity,
Ω', dimensional vorticity, ($m^3.s^{-2}$)

REFERENCES

[1]. S Shelyag, M Schüssler, SK Solanki, SV Berdyugina, A Vögler, G-band spectral synthesis and diagnostics of simulated solar magneto-convection, Journal of Astronomy & Astrophysics (A&A), 2004; 427: 335–343.

[2]. H Jamai, S O Fakhreddine, H Sammouda, Numerical Study of Sinusoidal Temperature in Magneto-Convection, Journal of Applied Fluid Mechanics, 2014; 7(3): 493-502.
[3]. M Sathiyamoorthy, C Ali, Effect of magnetic field on natural convection flow in a liquid gallium filled square cavity for linearly heated side walls, International Journal of Thermal Sciences, 2010; 49: 1856-1865.
[4]. R Zanella, C Nore, F Bouillault, X Mininger, J L Guermond, I Tomas, L Cappanera, Numerical study of the impact of magnetoconvection on the cooling of a coil by ferrouid, Non Linéaire Publications, Avenue de l'Université, BP 12, 76801 Saint-Etienne du Rouvray cedex ; 2017.
[5]. P Umadevi, N Nithyadevi, Magneto-convection of water-based nanofluids inside an enclosure having uniform heat generation and various thermal boundaries, Journal of the Nigerian Mathematical Society, 2016; 35: 82–92.
[6]. A Gelfgat, Y O Zikanov, Computational modeling of magneto-convection: Effects of discretization method, grid refinement and grid stretching. Computers and Fluids, 2018; 1–17.
[7]. J Sarr, C Mbow, H Chehouani, B Zeghmati, S Benet, M Daguenet, Study of Natural Convection in an Enclosure Bounded by Two Concentric Cylinders and Two Diametric Planes, Journal of Heat Transfer, 1995; 117: 130-137.
[8]. T Shin, Penetration of Alfvén waves into an upper stably-stratified layer excited by magnetoconvection in rotating spherical shells, Physics of the Earth and Planetary Interiors, 2015; 241: 37–43.
[9]. M L. Sow, J Sarr, C Mbow, B Mbow, B Claudet, M M Kane, Geometrical and Rayleigh Number Effects in the Transient Laminar Free Convection between Two Vertically Eccentric Spheres, International Journal of Numerical Methods for Heat & Fluid Flow, 2009; 19: 689-704.
[10]. L R Mack, H C Hardee, Natural Convection between Concentric Spheres at Low Rayleigh Numbers, International Journal of Heat and Mass Transfer, 1968; 11: 387-396.
[11]. M N Tazi, S Daoudi, G L Palec, M Daguenet, Numerical study of the Boussinesq model of permanent axisymmetric laminar natural convection in an annular space between two spheres, General Review of Thermal, 1997; 36: 239-251.
[12]. H A Rainer, A spectral solution of the magneto-convection equations in spherical geometry, International Journal for Numerical Methods in Fluids, 2000; 32: 773-797.
[13]. S Shelyag, M Schüssler, S K Solanki, A Vögler, Stokes diagnostics of simulated solar magneto-convection, Journal of Astronomy & Astrophysics (A&A), 2007; 469: 731–747.
[14]. P Dulal, C Sewli, Mixed convection magnetohydrodynamic Heat and mass transfer past a stretching surface in a micropolar fluid-saturated porous medium under the influence of ohmic heating, Soret and Dufour effects, Commun Nonlinear Sci Numer Simulat, 2011; 16:1329–1346.
[15]. S Das, S K Guchhait, R N Jana, O D Makinde, Hall effects on an unsteady magneto-convection and radiative heat transfer past a porous plate, Alexandria Engineering Journal, 2016; 55: 1321–1331.
[16]. H Ozoe, K Okada, The effect of the direction of the external magnetic field on the three-dimensional natural convection flow in a cubical enclosure, International Journal of Heat and Mass Transfer, 1989; 32: 1939-1954.
[17]. M Venkatachalappa, C K Subbaraya, Natural convection in a rectangular enclosure in the presence of magnetic field with uniform heat flux from side walls, Acta Mechanica, 1993; 96: 13-26.
[18]. P Dulal, Mixed convection heat transfer in the boundary layers on an exponentially stretching surface with magnetic field, Applied Mathematics and Computation. 2010; 217 (6): 2356-2369.
[19]. M N Koita, M L Sow, O N Thiam, V B Traoré, Mbow C, J Sarr, Unsteady Natural Convection between Two Eccentric Hemispheres, Open Journal of Applied Sciences, 2021; 11: 177-189.
[20]. A Vögler, S Shelyag, M Schüssler, F Cattaneo, T Emonet, T Linde, Simulations of magneto-convection in the solar photosphere, Journal of Astronomy & Astrophysics (A&A), 2004; 429: 335–351.